

Proceedings of the XVI National Conference on Superconductivity and Strongly Correlated Systems, Zakopane 2013

Phase Diagram and Activation Energy for Vortex Pinning in Nb/(Co,Pd) Superconductor–Ferromagnet Bilayer

Y. SYRYANY^a, M. ALESZKIEWICZ^a, MARTA Z. CIEPLAK^a, L.Y. ZHU^b AND C.L. CHIEN^b

^aInstitute of Physics, Polish Academy of Sciences, al. Lotników 32/46, 02-668 Warsaw, Poland

^bDepartment of Physics and Astronomy, The Johns Hopkins University, Baltimore, MD 21218, USA

Using the magnetoresistance measurements we study the phase transition line and the activation energy for vortex pinning in superconductor/ferromagnet bilayer, built of a ferromagnetic Co/Pd multilayer with perpendicular magnetic anisotropy, and a niobium film, with insulating layer in-between to eliminate proximity effect. The domain width is reversibly pre-defined using the angle-dependent demagnetization. We find that the enhancement of the activation energy for vortex pinning by magnetic domains is rather modest, by a factor of about 2.1. We attribute this to large domain width, and large dispersion of the domain width in this bilayer.

DOI: [10.12693/APhysPolA.126.A-123](https://doi.org/10.12693/APhysPolA.126.A-123)

PACS: 74.25.F-, 74.25.N-, 74.25.Wx, 74.62.-c, 74.70.-b, 74.78.-w, 74.78.Fk, 75.70.Kw, 75.70.-i

1. Introduction

Superconductor(S)–ferromagnet(F) bilayers (SFB) are a subject of many investigations, because they offer a chance to study the interactions between superconductivity and ferromagnetism [1–4]. Proximity effect occurs when the S and the F layers are in contact [4], while long-range, electromagnetic interactions may be induced by any magnetic domains existing in the F layer [1–3]. In the present work we focus on this last effect. It may be conveniently studied when proximity effect is cut off by inserting insulating layer between S and F layers.

The magnetic domains create inhomogeneous magnetic field which influences the dependence of the superconducting critical temperature, T_c , on the external magnetic field, H (phase transition line). When H is homogeneous, $T_c(H)$ is linear, with the maximum T_c at $H = 0$. In the presence of magnetic domains it becomes nonlinear, with the maxima shifted away from $H = 0$, as shown by theoretical [5–7] and experimental [8–10] studies. The magnetic domains are also very effective pinning centers for vortices, and attempts have been made to utilize this effect to enhance the critical current density [11–21]. Recently, we have demonstrated that large enhancement may be achieved, by a factor of more than 10, but this requires careful tuning of the magnetic domain pattern [22]. We have utilized a method of angled demagnetization to reversibly define and erase the quasi-periodic magnetic domain patterns with equal amount of $+/-$ domains, and tunable domain width, w . The experiment involved the SFB built of Co/Pt multilayer with perpendicular magnetic anisotropy (PMA) as the F layer, and niobium as the S layer [10, 22].

Surprisingly, the study of the pinning enhancement by magnetic methods in another SFB, built of Co/Pd multilayer with PMA and niobium, revealed disappointingly small enhancement [23]. In hope to understand the origins of this finding, here we study the magnetoresistance in similar SFB, with Co/Pd multilayer and thin Nb layer.

2. Experimental details

The SFB has been grown by sputtering at room temperature on a Si substrate, with the sequence of layers Si(10)/Pd(10)/[Co(0.5)/Pd(1.5)]_s/Si(10)/Nb(20)/Si(10), where the thickness is denoted in nanometers (Fig. 1a). The Si(10) layer between Co/Pd and Nb prevents proximity effect. The magnetic properties of the SFB are studied using superconducting quantum interference device (SQUID) magnetometer. The sample displays a square hysteresis loop in the normal state, characteristic for the PMA, with the coercive field at 300 K (10 K) of $H_c = 720$ Oe (1600 Oe). The electrical resistance R is measured by four-probe method, in the perpendicular magnetic field, using Physical Property Measurement System (Quantum Design). The sample, 1 mm wide and 5 mm long, with four contact pads along the long direction and more than 1.5 mm between the voltage contacts, is cooled just below the T_c , and the data are accumulated in T -increments of 2 to 3 mK.

Prior to resistance measurements the magnetic domain patterns are defined by demagnetization of the F layer at $T = 300$ K in the AC-magnetic field canted at an angle θ to the sample plane (Fig. 1d), and the domain patterns are imaged by magnetic force microscopy (MFM). Figure 1b,c shows two examples of MFM images, for SFB demagnetized at $\theta = 2^\circ$ and 90° . It is seen that the increase of θ dramatically increases the magnetic domains width. From MFM images we estimate the average domain width, w , and the standard deviation, Δw , as a function of θ . They are shown in Fig. 1e, where the error bars depict the magnitude of Δw . We observe a rapid increase of w , from $0.4 \mu\text{m}$ at $\theta = 0$ to $1.2 \mu\text{m}$ at $\theta = 20$, followed by a saturation for larger θ . In nominally the same Co/Pd multilayer, used in our previous study [23], we have seen larger range of w , 0.4 to $1.5 \mu\text{m}$. This is unavoidable sample-to-sample variation, resulting from very small layer thicknesses in the SFB. Nevertheless, the $w(\theta)$ dependence is qualitatively similar for

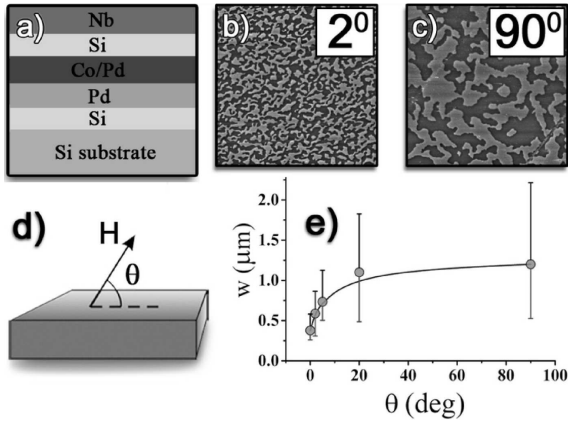


Fig. 1. (a) Schematic drawing of the SFB. (b,c) MFM images ($40 \mu\text{m} \times 40 \mu\text{m}$) at 300 K for SFB demagnetized at angles $\theta = 2^\circ$ and 90° , respectively. The dark (bright) color represents domains with positive (negative) magnetization. (d) The definition of the demagnetization angle θ . (e) Average domain width w versus θ . The error bars show the standard deviation, Δw .

these samples. It results from the fact that in the F layers with PMA the magnetic moment is out of plane in the uniform domain area, while it is in-plane in the domain walls. The in-plane demagnetizing AC field tends to align spins in-plane, and thus creates many domain walls and small w . With increasing θ the in-plane component of the AC field decreases, so larger domains are formed.

We have observed similar behavior in SFB's with Co/Pt multilayers [10, 22]. However, in that case w is smaller, in the range 0.3 to 0.7 μm , and Δw is small, about 10%. In contrast, in the Co/Pd multilayer studied presently Δw is large, between 40 to 50%. These differences are likely related to different thicknesses of the non-magnetic spacers in these multilayers, Pd and Pt, 1.5 nm and 0.3 nm, respectively. Different spacer thickness creates different density of structural defects, which affect domain formation during demagnetization.

3. Results and discussion

3.1. Phase transition line

Figure 2 shows the H -dependence of R/R_N , where R_N is the normal-state resistance at $T = 10$ K, for the F-layer demagnetized at $\theta = 90^\circ$ (a), and for saturated F-layer, labeled "s" (b). We observe that in the sF case the $R(H)$ dependence has one single minimum at $H = 0$, as expected when the magnetic field is homogeneous. On the other hand, two minima, situated at H between 50 and 90 Oe, are present in case of $\theta = 90^\circ$, signaling the presence of the inhomogeneous stray fields, as discussed previously [8–10].

Figure 3 shows the experimental phase boundaries extracted from the magnetoresistance, for the sF state, and for various θ , with the T_c defined at $R/R_N = 0.5$.

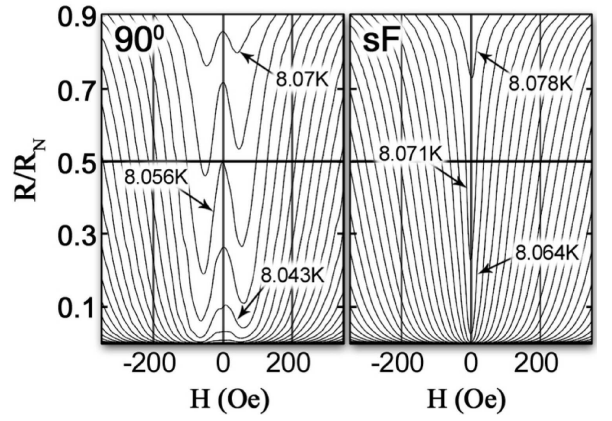


Fig. 2. R/R_N , resistance normalized to normal-state value at 10 K, versus H , in increments of 2–3 mK, for the F layer demagnetized at $\theta = 90^\circ$ (a) and for saturated F-layer (b).

The phase boundary $T_c(H)$ for the sF state is linear in H , with a single maximum of the T_c at $H = 0$. Using this result and the definitions of the coherence length in the dirty limit [24], $\xi(T) = \xi(0)/\sqrt{1 - T/T_{c0}}$, and the upper critical field $H_{c2}(T) = \Phi_0/2\pi\xi^2(T)$, where $\Phi_0 = 20.68 \text{ G}\mu\text{m}^2$ is the flux quantum, we estimate $T_{c0} = 8.074 \text{ K}$ and $\xi(0) \approx 10.73 \text{ nm}$.

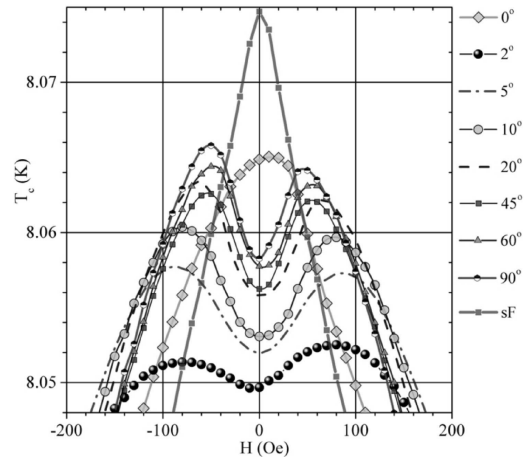


Fig. 3. The $T_c(H)$ for the SFB after demagnetization at various θ , and for the sF state.

The $T_c(H)$ becomes nonlinear in the presence of magnetic domains. As shown in Fig. 3 it evolves with increasing θ , from the dependence having a single maximum in the vicinity of $H = 0$ for $\theta = 0^\circ$, to the one with two maxima away from $H = 0$ for every other value of θ . The positions of the maxima drift with increasing θ , from $H \approx 90$ Oe for $\theta = 2^\circ$, to $H \approx 50$ Oe for $\theta = 90^\circ$. The T_c at the maximum, T_c^{max} , is initially suppressed when θ increases from 0 to 2° , but further increase of θ results in the gradual regain of the T_c^{max} value to the one observed at $\theta = 0$. At $\theta = 2^\circ$, when the suppression of the T_c^{max}

is the largest, the average domain width is $w = 0.58 \mu\text{m}$ and $T_c^{\text{max}} = 8.052 \text{ K}$, which corresponds to $w \simeq 2.8\xi$.

These features are in qualitative agreement with the results discussed in the case of SFB with Co/Pt multilayer [10]. They are also in approximate agreement with numerical calculations for SFB with 1-dimensional (1D) periodic stripe domain pattern [7]. The explanation is as follows. The local magnetic field above domain is $B_{\text{loc}} = H + B_z$, where B_z is the domain stray field. When the SFB is cooled down, the superconductivity is nucleated first in the areas, in which H compensates B_z , so that $B_{\text{loc}} = 0$. When the domains are wide, $w > 2\xi$, this occurs above domain centers, for negative (positive) H above positively (negatively) charged domains, resulting in two maxima of the T_c . With increase of w the B_z at the domain center decreases [25]. Therefore, both the magnitude of compensating field, and the suppression of the T_c^{max} , are reduced. When the domains are narrow, $2w \ll \xi$, the nucleation is expected in the area extending above several domains, in an averaged stray field, resulting in a single T_c^{max} at $H = 0$. Strictly speaking, in our experiment this regime does not occur, because at $\theta = 0$ we have $w \gtrsim \xi$. However, the large dispersion of w in our SFB most likely causes averaging of the stray fields, and results in a single broad maximum at $H = 0$.

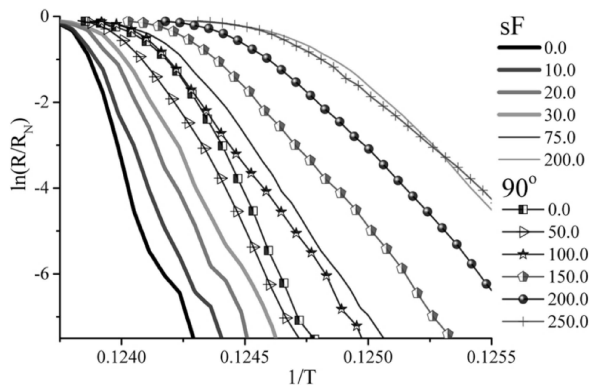


Fig. 4. The Arrhenius plots of $\ln(R/R_N)$ vs. $1/T$ for sF state (continuous lines) and for $\theta = 90^\circ$ (points and lines) for several magnetic fields (labeled in Oe).

3.2. Activation energy for vortex pinning

To understand how the magnetic domains affect the pinning of vortices, we analyze the dependence of $\ln(R/R_N)$ on $1/T$ for various H and θ . Figure 4 shows selected set of data for sF state, and for $\theta = 90^\circ$. At low T the data follow linear dependences, indicating that the Arrhenius law is obeyed. While the slope of these dependences changes monotonically with increasing H for sF state, the change is not monotonous for $\theta = 90^\circ$. Following the previous treatments of the flux activation regime [10, 26], we fit the linear portions by the dependence $\ln(R/R_N) = -U_0(H)/(k_B T) + K(H)$. Here U_0 is the zero-temperature flux activation energy,

and $K(H)$ is the coefficient in the T -dependent term, so that the general form for the activation energy is $U(T, H) = U_0(H) - K(H)T$.

Figure 5 shows the dependence of U_0 on H (on a logarithmic scale) for the sF state and for several values of θ . The error bars indicate the standard deviation, ΔU_0 , extracted from the fits to the Arrhenius plots. The magnitude of ΔU_0 is reasonably small (about 16%) for most values of θ , but it is large, more than 50%, for $\theta = 0$, reflecting the deviations of the data from linearity. Such deviations suggest that in this case the single U_0 value cannot be defined.

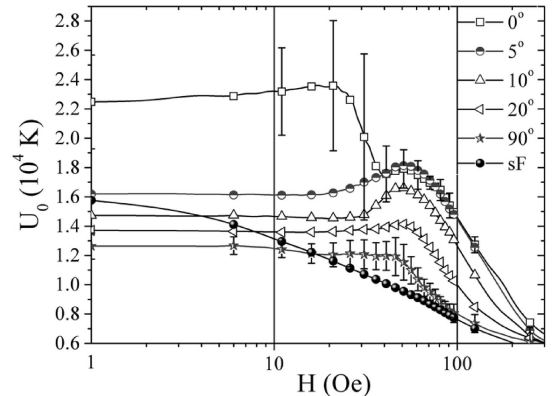


Fig. 5. Activation energy U_0 versus H for different magnetic states of the SFB structure. The error bars (drawn for clarity for some selected points only) indicate standard deviation extracted from the fits to the Arrhenius plots.

Furthermore, we see that in the sF state the U_0 is proportional to $\ln H$, as has been reported for thin niobium films [26], and attributed to the distribution of pinning strength, and filling of the strongest pinning centers. We have also observed a similar behavior in the sF state of the SFB with Co/Pt [10]. On the other hand, in the SFB with predefined magnetic domains the logarithmic dependence on H is absent. Instead, we may identify three regions with different behavior of $U_0(H)$. In the region I, at $H \lesssim 20$ Oe, U_0 is H -independent, and for $\theta = 0$ it is by a factor of about 1.5 larger than in the case of sF state. However, U_0 decreases with increasing θ , indicating that with increasing w the enhancement of pinning gradually changes into suppression. In the region II, for $20 \text{ Oe} \lesssim H < 100 \text{ Oe}$, broad maxima appear. We see two maxima for $\theta = 0$, situated at $H_1 \approx 20$ Oe, and at $H_2 \approx 55$ Oe. For every other θ there is only one maximum, at H_2 , with the magnitude of H_2 decreasing slightly with increasing w . Finally, in the region III, at $H > 100$ Oe, the U_0 gradually approaches the curve observed for the sF state.

Many of these features are similar to those observed and discussed previously for SFB with Co/Pt multilayer [10]. The gradual decrease of U_0 in region III likely results from the vortex density exceeding the density of the pinning centers. The broad maxima in region

II suggest commensurability effects between the vortex lattice and the pinning potential created by domains. In the SFBs, depending on w , various vortex configurations above the domains are possible, including disordered Abrikosov lattice, or 1D and 2D vortex chains [10]. The detailed discussion of these possibilities is beyond the scope of the present paper and will be presented elsewhere. We would like to stress that the broadness of the maxima observed here suggests that vortex configurations are spatially limited, which directly results from large magnitude of Δw . Finally, the H -independent U_0 in region I is most likely caused by the enhanced vortex flow along magnetic domains at small H , when the vortex density is low. The vortex flow increases with increasing w leading to the suppression of the flux pinning at large domain width.

Turning now to comparison between two types of SFBs, with Co/Pd studied here, and with Co/Pt reported in Refs. [10, 22], we note that the largest enhancement of U_0 observed in the present experiment equals to about 2.1. It is seen for the smallest w , and in the vicinity of the first maximum on $U_0(H)$ curve, at about 20 Oe. In case of Co/Pt multilayer qualitatively similar situation occurs, except that maximum enhancement of U_0 is larger, about 3.3, and the first maximum on U_0 curve is located at larger H , at about 100 Oe [22]. It appears that both larger w , and larger Δw in the case of Co/Pd multilayer are responsible for smaller enhancement of U_0 . Larger w leads to smaller value of the commensurability field at which maximum of U_0 occurs, and results in smaller vortex density which is pinned at this field. Moreover, larger Δw limits the spacial area of the pinning, which further reduces the density of pinned vortices.

In conclusion, we have studied the magnetoresistance in the SFB built with Co/Pd multilayer and niobium. We use angled demagnetization method to tune magnetic domain width which allows mapping out the influence of the domain width on the phase boundary $T_c(H)$, and on the activation energy for the vortex pinning, U_0 . The largest enhancement of U_0 is observed for smallest w , similarly as it has been reported for SFB with Co/Pt multilayer. However, the enhancement of U_0 induced by magnetic domains is smaller in case of Co/Pd, which appears to be caused by larger domain width, and larger dispersion of the domain width.

Acknowledgments

This work was supported by Polish NSC grant 2011/01/B/ST3/00462, by the European Union within the ERDF through Innovative Economy grant POIG. 01.01.02-00-108/09, and by NSF grant DMR 0821005. The research was partially performed in the NanoFun laboratories co-financed by the ERDF project POIG.02.02.00-00-025/09.

References

[1] I.F. Lyuksyutov, V.L. Pokrovsky, *Adv. Phys.* **54**, 67 (2004).

[2] M. Velez, J.I. Martín, J.E. Villegas, A. Hoffmann, E.M. González, J.L. Vicent, Ivan K. Schuller, *J. Magn. Magn. Mater.* **320**, 2547 (2008).

[3] A. Yu. Aladyshkin, A.V. Silhanek, W. Gillijns, V.V. Moshchalkov, *Supercond. Sci. Technol.* **22**, 053001 (2009).

[4] A.I. Buzdin, *Rev. Mod. Phys.* **77**, 935 (2005).

[5] A.I. Buzdin, A.S. Mel'nikov, *Phys. Rev. B* **67**, 020503(R), (2003).

[6] A. Yu. Aladyshkin, A.I. Buzdin, A.A. Fraerman, A.S. Mel'nikov, D.A. Ryzhov, A.V. Sokolovet, *Phys. Rev. B* **68**, 184508 (2003).

[7] A. Yu. Aladyshkin, V.V. Moshchalkov, *Phys. Rev. B* **74**, 064503 (2006).

[8] Z. Yang, M. Lange, A. Volodin, R. Szymczak, V.V. Moshchalkov, *Nature Mater.* **3**, 793 (2004).

[9] W. Gillijns, A.Yu. Aladyshkin, M. Lange, M.J. Van Bael, V.V. Moshchalkov, *Phys. Rev. Lett.* **95**, 227003 (2005); W. Gillijns, A. Yu. Aladyshkin, A.V. Silhanek, V.V. Moshchalkov, *Phys. Rev. B* **76**, 060503(R) (2007).

[10] L.Y. Zhu, Marta Z. Cieplak, C.L. Chien, *Phys. Rev. B* **82**, 060503(R) (2010).

[11] L.N. Bulaevskii, E.M. Chudnovsky, M.P. Maley, *Appl. Phys. Lett.* **76**, 2594 (2000).

[12] A. Garcia-Santiago, F. Sanchez, M. Varela, J. Tejada, *Appl. Phys. Lett.* **77**, 2900 (2000).

[13] X.X. Zhang, G.H. Wen, R.K. Zheng, G.C. Xiong, G.J. Lian, *Europhys. Lett.* **56**, 119 (2001).

[14] M. Lange, M.J. Van Bael, V.V. Moshchalkov, Y. Bruynseraede, *Appl. Phys. Lett.* **81**, 322 (2002).

[15] D.B. Jan, J.Y. Coulter, M.E. Hawley, L.N. Bulaevskii, M.P. Maley, Q.X. Jia, B.B. Maranville, F. Hellman, X.Q. Pan, *Appl. Phys. Lett.* **82**, 778 (2003).

[16] M.Z. Cieplak, X.M. Cheng, C.L. Chien, Hai Sang, *J. Appl. Phys.* **97**, 026105 (2005).

[17] M.Z. Cieplak, Z. Adamus, A. Abal'oshev, I. Abal'osheva, M. Berkowski, X.M. Cheng, Hai Sang, C.L. Chien, *Phys. Status Solidi C* **2**, 1650 (2005).

[18] M. Feigensohn, L. Klein, M. Karpovski, J.W. Reiner, M.R. Beasley, *J. Appl. Phys.* **97**, 10J120 (2005).

[19] V. Vlasko-Vlasov, U. Welp, G. Karapetrov, V. Novosad, D. Rosenmann, M. Iavarone, A. Belkin, W.-K. Kwok, *Phys. Rev. B* **77**, 134518 (2008).

[20] A. Belkin, V. Novosad, M. Iavarone, J. Pearson, G. Karapetrov, *Phys. Rev. B* **77**, 180506 (2008).

[21] V.K. Vlasko-Vlasov, U. Welp, A. Imre, D. Rosenmann, J. Pearson, W.K. Kwok, *Phys. Rev. B* **78**, 214511 (2008).

[22] M.Z. Cieplak, L.Y. Zhu, Z. Adamus, M. Kończykowski, C.L. Chien, *Phys. Rev. B* **84**, 020514(R) (2011).

[23] Y. Syryanyy, L.Y. Zhu, M.Z. Cieplak, C.L. Chien, *Acta Phys. Pol. A* **118**, 399 (2010).

[24] M. Tinkham, *Introduction to Superconductivity*, Dover, New York 2004.

[25] G.M. Maksimova, R.M. Ainbinder, D.Y. Vodolazov, *Phys. Rev. B* **78**, 224505 (2008).

[26] J.W.P. Hsu, A. Kapitulnik, *Phys. Rev. B* **45**, 4819 (1992).